Curcumin-loaded nanocomplexes alleviate the progression of fluke-related cholangiocarcinoma in hamsters

Chanakan Jantawong
Khon Kaen University
Yaovalux Chamgramol
Khon Kaen University
Kitti Intuyod
Khon Kaen University
Aroonsri Priprem
Mahasarakham University
Chawalit Pairojkul
Khon Kaen University
Rungtiwa Dangtakot
Nakhonratchasima College
Thatsanapong Pongking
Khon Kaen University
Porntip Pinlaor
Khon Kaen University
Sakda Waraasawapati
Khon Kaen University
Somchai Pinlaor (psomec@kku.ac.th)
Khon Kaen University

Research Article

Keywords: nanoencapsulated curcumin, Opisthorchis viverrini, liver fluke infection, bile duct cancer, cholangiofibrosis, cholangiofibroma

Posted Date: April 7th, 2022

DOI: https://doi.org/10.21203/rs.3.rs-1519303/v1

Additional Declarations: No competing interests reported.

Version of Record: A version of this preprint was published at Cancer Nanotechnology on January 24th, 2023. See the published version at https://doi.org/10.1186/s12645-023-00155-0.

Abstract

Background: Curcumin-loaded nanocomplexes (CNCs) previously demonstrated lower toxicity and extended release better than is the case for free curcumin. Here, we evaluated the efficacy of CNCs against opisthorchiasis-associated cholangiocarcinoma (CCA) in hamsters.

Method: Dose optimization (dose and frequency) was performed over a one-month period using hamsters, a model that is widely used for study of opisthorchiasis-associated cholangiocarcinoma. In the main experimental study, CCA was induced by a combination of fluke, *Opisthorchis viverrini* (OV), infection and *N*-nitrosodimethylamine (NDMA) treatment. Either blank (empty) nanocomplexes (BNCs) or different concentrations of CNCs (equivalent to 10 and 20 mg cur/kg bw) were given to hamsters thrice a week for five months. The histopathological changes, biochemical parameters, and the expression of inflammatory/ oncogenic transcription factors were investigated.

Results: The optimization study revealed that treatment with CNCs at a dose equivalent to 10 mg cur/kg bw, thrice a week for one month, led to a greater reduction of inflammation and liver injury induced in hamsters by OV+NDMA than did treatments at other dose rates. Oral administration with CNCs (10 mg cur/kg bw), thrice a week for five months, significantly increased survival rate, reduced CCA incidence, extent of tumor development, cholangitis, bile-duct injury and cholangiofibroma. In addition, this treatment decreased serum ALP and ALT levels and suppressed expression of oncogenic transcription factors including NF- κB and FOXM1.

Conclusion: CNCs (10 mg cur/kg bw) attenuate the progression of fluke-related CCA in hamsters.

Background

Cholangiocarcinoma (CCA), a primary carcinoma of the intrahepatic bile duct, is generally a rare cancer. However, it has been frequently reported among oriental populations who are endemically infected with the liver flukes, *Opisthorchis viverrini* (OV) (Waraasawapati et al. 2021) or *Clonochis sinensis*, in parts of the Greater Mekong Sub-region countries (Shin et al. 2010; Sirica et al. 2019). Northeast Thailand has the highest risk of all, with an annual incidence rate of 90 per 100,000 person-years in males and 38.3 per 100,000 person-years in females (Sriamporn et al. 2004). In Northeast Thailand, OV infection is acquired by eating popular simple dishes; marinated chopped raw fish or a short-pickled fish, preparations from freshwater fish which contains the infective stage of OV in tissue (Prueksapanich et al. 2018). Moreover, people in northeastern Thailand are also exposed to a carcinogen (i.e., nitrosamine) in favorite fermented fish (Mitacek et al. 1999). Thus, traditional eating habits on a daily basis result in a local population repeatedly exposed to both OV infection and nitrosamine-contaminated food from early in life.

Synergistic effects of nitrosamines and OV infection induce CCA in Syrian golden hamsters, under conditions whereby the administration of chemical carcinogen or fluke infection alone do not cause cancer (Thamavit et al. 1987). In this carcinogenesis model, chronic inflammation in response to chronic infestation by liver flukes results in release of cytokines and growth factors leading to biliary cell proliferation (Sripa et al. 2018; van Tong et al. 2017; Yongvanit et al. 2012). At the same time, nitrosamines act as xenobiotics and stimulate hyperplasia of oval cells (hepatic stem/progenitor cells) and develop atypical ductular proliferation. The proliferation of oval cells by liver cell injury is suspected to be early progenitor cells for hepatocytes and bile duct cells origin to cause cholangiofibrosis, cholangiofibroma, hepatocellular and/or cholangiocellular carcinomas (cholangiocarcinoma, CCA) (Chen et al. 2019; Lee et al. 1997). Based on case series, epidemiological data, and experimental animal models, the international Agency for Research on Cancer have classified OV and *C. sinensis* as class 1 carcinogen in humans (IARC 2012).

Oncogenesis of CCA in fluke-associated tumors is initiated by oxidation/nitration of DNA damage (Banales et al. 2020; Yongvanit et al. 2012). Upregulation of inflammation-associated transcription factors, e.g. nuclear factor kappa (NF-κB) and activator protein 1 (AP-1), as well as their downstream targets such as inducible nitric oxide synthase (iNOS) and cyclooxygenase-2 (COX-2), have been identified both in animal models (Prakobwong et al. 2010) and clinical samples (Pinlaor et al. 2005). Upregulation of NF-κB (Dolcet et al. 2005), forkhead box m1 (FOXM1) (Wierstra 2013) and high mobility group box 1 (HMGB1) (Vijayakumar et al. 2019) are involved in inflammation-associated carcinogenesis and targeted for cancer therapy. Hence, discovery of agents that exert anti-inflammatory and anti-infection effects and that can attenuate cholangiofibrosis could lead to alternative treatments for CCA.

Compounds derived from herbs have been extensively studied and proposed as alternative treatments for several cancers. Curcumin, a yellow pigment derived from the rhizome of *Curcuma longa*, is one of the most-studied natural compounds for cancer treatment. It exerts several health-beneficial properties particularly anti-inflammatory, anti-infection and also anti-fibrosis activities (Razavi et al. 2021). Curcumin is a promising agent for prevention and treatment of cancers in animal models including *O. viverrini*-associated CCA (Pinlaor et al. 2009; Prakobwong et al. 2011b), and clinical trials of curcumin has been introduced for many cancer types (Mansouri et al. 2020; Shehzad et al. 2010). However, curcumin has several unfavorable properties, especially poor water solubility, low bioavailability and it is prone to degradation (Liu et al. 2016), limiting its activity in clinical trials (Anand et al. 2007; Baker 2017). Efforts have therefore been made to overcome these unfavorable properties (Mahran et al. 2017; Rafiee et al. 2019; Zhang et al. 2019).

One of the approaches is incorporation of curcumin into nanocarrier systems such as lipid-based nanocarriers, polymer-based nanocarriers, hydrogels, dendrimers and so on (Ipar et al. 2019; Rafiee et al. 2019; Zhang et al. 2019). Incorporation of curcumin into a mucoadhesive polymeric nanocarrier to deliver this payload into the gastrointestinal tract has been particularly promising (Suwannateep et al. 2011). Polymeric nanocurcumin has recently been improved by covering particles with xanthan and arabic gums—so-called curcumin-loaded nanocomplexes (CNCs) (Pinlaor S et al. 2021). CNCs have very low toxicity for biliary epithelial cells and exhibit anti-CCA activity against CCA cell lines (Pinlaor S et al. 2021). Similarly, CNCs have very low acute and chronic toxicity in animal models (Jantawong et al. 2021). However, attenuation of progression of CCA by CNCs *in vivo* has not yet been demonstrated.

The objective of this study was to assess the effect of a five-month regimen of treatment with CNCs against CCA induced in a hamster model by *O. viverrini* infection. In this model, there is poor prognosis due to multi-site metastasis. Assessment of animal survival, number of tumors, histopathological changes,

biochemical parameters, and the expression of inflammatory/oncogenic transcription factors were all investigated to assess the attenuation efficacy of CNCs on tumor development. This preclinical study should be a basis for translation to eventual clinical use.

Materials And Methods

Chemicals and reagents

Curcumin (> 98% purity w/w) was purchased from ACROS Organics (Geel, Belgium). ECL™ Prime Western blotting detection reagent and polyvinylidene difluoride (PVDF) membrane were purchased from GE Healthcare (Piscataway, NJ, USA). Rabbit anti-FOXM1 (C-20) was obtained from Santa Cruz (Dallas, Texas, USA). Horseradish peroxidase (HRP)-conjugated secondary antibody was purchased from Jackson ImmunoResearch (West Grove, PA, USA). Rabbit anti-β-actin, p65, RIPA buffer and bovine serum albumin were purchased from Cell Signaling Technology (Danvers, MA, USA). Rabbit anti-CK-19, anti-AFP, anti-HMGB1 and anti-PCNA were purchased from Abcam (Cambridge, MA, USA).

Preparation of CNCs

Curcumin-loaded nanocomplexes (CNCs, WellCap® Kaminn, Encapsulation efficiency = 80%, Loading capacity = 28%, particle size 400–1,000 nm) and blank nanocomplexes (BNCs, WellCap® Capsule) powder were obtained from Welltech Biotechnology Co. Ltd. Bangkok, Thailand. CNCs were prepared according to a previously described spray-drying method (Pinlaor S et al. 2021).

Animals

Male Syrian golden hamsters (*Mesocricetus auratus*) (n = 100), 4-6-weeks old, weight 80–100 g, were obtained from the Animal Unit at the Faculty of Medicine, Khon Kaen University, Khon Kaen, Thailand. Animals were randomly selected and kept in their cages for at least 5 days before the start of the experiment. All animals were maintained under clean conventional conditions at 23°C (± 2°C) with relative humidity 30–60% and 12 h light/dark cycle. The animals were provided *ad libitum* a commercial pellet diet (CP-SWT, Thailand) with unlimited supply drinking water. To avoid bacterial contamination, the stainless-steel cages were washed once a week with Sunlight detergent (Unilever, Thailand), decontaminated using the antimicrobial reagent Dettol (Dettol, Thailand) and sawdust was changed twice per week.

Isolation of **Opisthorchis viverrini** metacercariae

Opisthorchis viverrini metacercariae were isolated from naturally infected cyprinid fishes by pepsin digestion as described previously (Pinlaor et al. 2009). Briefly, fishes were digested in 0.25% pepsin-1.5% HCl (Wako Pure Chemical Industries, Osaka, Japan) in 0.85% NaCl solution and *O. viverrini* metacercariae were isolated and counted. Viable cysts were used to infect hamsters. Fifty *O. viverrini* metacercariae were given to each hamster by intragastric gavage. *N*-nitrosodimethylamine (NDMA) was given as 12.5 ppm in drinking water.

Experimental design

Preliminary study on CNCs dose optimization

Nanoparticles are known to increase the oral bioavailability of curcumin (Zhang et al. 2019). The effective dose of curcumin in CNCs was firstly performed to optimize for the main experimental study according to our previous report (Prakobwong et al. 2011b). Ten hamsters were randomly divided into five groups: (1) normal control (Normal, n = 2); (2) *O. viverrini* (OV) infection plus NDMA without any treatment (ON, n = 2); (3–5), OV plus NDMA and treated with 35.71, 71.43 and 142.86 mg/kg/bw of CNCs (equivalent to 10, 20, and 40 mg cur/kg bw), respectively (ON + CNCs, n = 2 each). Hamsters were infected with 50 *O. viverrini* metacercariae and one week later they were given NDMA together with CNCs (thrice a week) for a subsequent one month.

Experimental animals used to determine the effect of CNCs on progression of CCA

Ninety hamsters were divided into five groups: (1) normal control (Normal, n = 20); (2) a combination of *O. viverrini* (OV) infection and NDMA without any treatment (ON, n = 30); OV plus NDMA followed by administration of BNCs (3)(ON + BNCs, 71.43 mg/kg bw, n = 10), or CNCs (4) 35.71 mg/kg (ON + CNCs, equivalent to 10 mg cur/kg bw, n = 15) or (5) CNCs 71.43 mg/kg (ON + CNCs, equivalent to 20 mg cur/kg bw, n = 15).

One week after infection with *O. viverrini* metacercariae, hamsters were given CNCs or BNCs thrice a week for five months. NDMA solution (12.5 ppm) was added to water, which animals were allowed to access *ad libitum*, for the first two months of the experiment. Body weights were recorded weekly. After the end of the experiment, all animals were starved for one day before being euthanized.

Sample collection

At the end of the study, hamsters were anesthetized and euthanized by isoflurane inhalation. Blood and liver tissue were collected. For the preliminary experiment to determine the optimal dose of CNCs, only biochemical parameters, liver weight to body weight ratio and histopathology were analyzed. Tumor volumes (TV) were measured using formula TV = (length x width^2)/2, where length represents the longest diameter of the tumor and width represents the smallest diameter of the tumor (Carlsson et al. 1983). Blood was collected by cardiac puncture and placed into clotted blood tubes and centrifuged at 3,500 rpm at 4°C for 10 min. Serum was separated and aliquoted and kept at -20°C until used for measurement of biochemical parameters. For histopathology and immunohistochemical tests, liver tissues were collected and fixed in 10% buffered formalin. For western-blot analysis, liver samples were collected in liquid nitrogen as snap-frozen samples and kept at -20°C until used.

Biochemical measurement

Activities of liver function enzymes and levels of other biochemical parameters in serum of hamsters were measured using a Cobas 8000 Chemistry Autoanalyzer (Roche Diagnostics International Ltd., Scotland). The data were reported as means ± SD.

Histopathology

Liver tissues were fixed in 10% buffered formalin and paraffin-embedded sections were cut at 4 μm thickness and stained with hematoxylin and eosin (H&E) as well as with alcian blue/PAS for mucins. The grading approach for classifying inflammatory responses, both in terms of distribution and quantity, followed the International Harmonization of Nomenclature and Diagnostic Criteria for Lesions in Rats and Mice (INHAND) (Thoolen et al. 2010). Cholangiofibrosis, cholangiofibroma and CCA lesions were assessed on all lobes of the liver. Cholangiofibrosis is a specific ductular reaction originating from initial oval-cell hyperplasia in response to pronounced hepatic parenchyma necrosis (Narama et al. 2003; Thoolen et al. 2010). Chronic active inflammation grades were based on the degree of neutrophilic and mononuclear inflammatory-cell infiltration, and of inflammatory-cell exudates in bile-duct lumens, portal interstitial tissue or adjacent liver parenchyma. Scores are presented separately for both perihilar bile duct and peripheral bile duct as follows: grade 0, no cholangitis: grade 1, marginal cholangitis: grade 2, slight cholangitis: grade 3, moderate cholangitis, grade 4, marked cholangitis and grade 5, severe cholangitis (Thoolen et al. 2010). Grading scores and pathology diagnosis were assigned in a double-blind manner by at least two independent researchers.

Immunohistochemistry

Liver sections (4-μm thickness) from all main experimental groups were subjected to immunohistochemistry. Rabbit anti-CK19 (1:100; ab15463, Abcam, UK), rabbit anti-AFP (1:500, GA500, Dako Omnis, USA), rabbit anti-PCNA (1:1000, ab2426, Abcam, UK) and rabbit anti-HMGB1 (1:350 ab79823, Abcam, UK) were used in 1% fetal bovine serum (FBS) overnight in a humidified chamber at 4°C. After washing with phosphate-buffered saline solution, slides were incubated with a 1:200 dilution of horseradish peroxidase (HRP)-labeled goat anti-rabbit IgG for 1 h at room temperature. The immunoreactivity signal was generated using diaminobenzidine substrate and the sections were counterstained with Mayer's hematoxylin and assessed using light microscopy. Ten fields (200× magnification) of each slide were randomly selected and an image captured using a Nikon E600 microscope, Melville NY, USA. Grading of each image was done by three separate researchers. The percent positive area (blue stack) was quantified using ImageJ software (National Institutes of Health, Bethesda, MD, USA) (Bai et al. 2016).

Western blot analysis

Twenty to 40 μg of protein extracted from each hamster liver was separated by sodium dodecyl sulfate polyacrylamide-gel electrophoresis (SDS-PAGE*)*, 7% separating gel, 5% stacking gel and then transferred to a poly vinylidene fluoride (PVDF) membrane. The membranes were probed with 1:1000 dilutions of primary antibodies against either rabbit anti-NF-kB (cat. no. ab7970, Abcam, UK), rabbit anti-FOXM1 (C-20, obtained from Santa Cruz Biotechnology (Santa Cruz, CA, USA)) or mouse anti-β-actin (cat. no. ab 3280, Abcam, UK) at 4°C overnight. After washing with 0.05% PBS-T, membranes were incubated with HRP-conjugated secondary antibody (1:3000) at room temperature for 1 h. Reactive bands were detected using chemiluminescence (ECL Plus, GE Healthcare). The intensity of reaction bands was quantified using the ImageJ open platform software, https://imagej.nih.gov/ij/plugins/ (NIH, Bethesda, MD).

Statistical analysis

Survival rate of hamsters was analyzed using Kaplan-Meier analysis. Graded scores of the stained tissue sections were compared using the non-parametric Mann-Whitney U test, using IBM SPSS statistics, version 23. The data are reported as means ± S.D. To compare different experimental conditions, data were analyzed using analysis of variance (one-way ANOVA) along with post-hoc tests. *P*-values of < 0.05 were considered to be statistically significant.

Results

Optimization for the effective dose and timing of curcumin content in CNCs

We first optimized the dose and the frequency of treatment. An oral daily administration with CNCs 50 mg cur/kg bw for five months was firstly evaluated as previous demonstrated in suppression of CCA-induced by OV + NDMA. The result showed that animals had a poor survival rate when compared with administration thrice a week as in Fig. S1. Thus, we reduced the CNCs dose and treated animals thrice a week for the main experiment. All hamsters survived administration of CNCs (equivalent to 10, 20 and 40 mg cur/kg bw) thrice a week for 1 month, and some biochemical assays including globulin, direct bilirubin levels and ALT trended to decrease when compare with the ON group. In particular, AST yielded values significantly lower than in the ON group, indicating that CNCs can prevent liver injury. Notably, these biochemical parameters were significantly lower in the groups treated with CNCs 10 and 20 mg cur/kg bw thrice weekly than in those dosed at 40 mg cur/kg bw (Table S1). The liver was brown without gross tumor lesions apparent at any dose rate. Reduction of inflammation was much greater after treatment with 10 and 20 mg cur/ kg bw than with 40 mg cur/ kg bw (Fig. S2A). Body weight gain (Fig. S2B), body weight before and after the experiment (Fig. S2C) and liver-weight to body-weight ratio (Fig. S2D) did not differ significantly among all experimental groups. Thus, CNCs doses of 10 and 20 mg cur/kg bw, administered three times a week were chosen for further experimental investigation.

CNCs increase survival of animals with CCA

After 5 months (159 days), 95% (19/20) of hamsters in the control group were still alive (Fig. 1). Survival rate of animals in the ON, ON + BNC and ON + CNCs (both concentrations) groups were significantly lower than in the controls. In the ON group, survival rate was 40% (12/30). Survival rates were significantly higher in groups given CNCs at dosages of curcumin equivalent to 10 and 20 mg cur/kg bw; 66.67% (10/15) and 53.33% (8/15), respectively. In the ON + BNC group, the survival rate was 40% (4/10), which was similar to that in the ON group (Fig. 1).

CNCs reduce macroscopic lesion appearance and improve body weight and liver-weight to body-weight ratio

Gross pathology of hamster livers are shown in Fig. 2A. The largest tumor mass with multiple white spots was seen in ON and ON + BNC groups, but fewer lesions were present in ON + CNCs 10 and 20 mg cur/kg bw.

Body weight gains were lower than normal controls in the ON group and in the two ON + CNCs groups, but higher in the BNC treatment group. The body weight gain in the ON group was significantly lower than in the BNC group, as shown in Fig. 2B. Relative body weight had increased significantly in all experimental groups by the end of the experiment (Fig. 2C). In addition, liver-weight to body weight ratio among ON, ON + BCN and ON + CNCs (both concentrations) groups were all similar and were significantly higher than normal hamsters (Fig. 2D).

CNCs alter biochemical parameters associated with liver injury

Table 1 shows the effects on biochemical parameters after oral administration with CNCs thrice a week for five months in hamsters with ON-induced CCA. Although total protein did not much change in all experimental conditions, levels of albumin had significantly decreased and levels of globulin, total bilirubin and ALT had significantly increased in ON, ON + BNC and ON + CNCs (both concentrations) groups relative to normal controls. The greater serum AST levels in ON, ON + BNC and ON + CNCs (both concentrations) groups were all similar and did not significantly differ from levels in the normal control group. Serum alkaline phosphatase level was significantly higher than in controls in the ON group, but its level was reduced after CNCs treatment (10 and 20 mg cur/kg bw). Unexpectedly, the level of alkaline phosphatase in the BNC treatment group was comparable to that in the CNCs treatment groups.

CNCs delay tumor development and attenuate the severity of liver histopathological changes in livers

Fifty percent of hamsters (6/12) developed CCA in the ON group and 50% (2/4) in the ON + BNC group. In the ON + CNCs 10 mg cur/kg bw group, 30% of hamsters (3/10) developed CCA. Unexpectedly, 75% (6/8) hamsters in the ON + CNCs 20 mg/kg bw group developed CCA, suggesting that adverse effects may have resulted from an overdose of curcumin. Tumor mass in hamster liver was measured and presented as tumor volumes (mm^3). Hamsters in the ON + BNC group and the ON + CNCs (both concentrations) groups had lower tumor volumes than the ON group. This was especially marked in the ON + CNCs 10 mg cur/kg bw group (Table 2).

The existence of CCA was also confirmed by H&E staining. In agreement with gross pathology, the ON group had the highest number of hamsters with cancer. Recurrent ascending cholangitis is common in chronic cholestasis found in hamsters infected with *O. viverrini*. A combination of acute and chronic inflammatory cells in bile ducts, periductal tissue and adjacent liver tissue was considered as chronic active inflammation (Thoolen et al. 2010). Figure 3 demonstrate chronic cholestasis due to chronic *O. viverrini* infection with chronic active inflammation and healing cholangitis, leading to occasional cholangiofibrosis. Histopathological changes in all experimental groups are summarized in Table 2. Cholangiofibrosis appears as minute grayish granules in the parenchyma. The lesion consists of hyperplastic bile ductules, intestinal metaplasia foci and fibrotic stroma (Fig. 4). Cholangiofibroma is an expanded nodule-forming cholangiofibrosis that appears as gray nodular or multinodular lesions with distinct borders and may compress adjacent liver tissue (Fig. 4). CCA shows as a grayish-white focal liver mass or cluster of nodules or plaque. It is an adenocarcinoma, composed of glands, solid sheets, trabeculae or closely packed ductules, with or without production of mucin (Fig. 5).

In the ON group, greater active inflammation, cholangiofibroma and tumor mass were clearly observed. The ON + BNC group showed similar histological findings to the ON group. In contrast, these histopathological changes were less pronounced in the CNCs treatment group at 10 mg cur/kg bw, but this group exhibited increased cholangiofibrosis. Notably, hamsters treated with CNCs at 20 mg cur/kg bw exhibited more cholangiofibroma and higher tumor mass than did the hamsters treated with 10 mg cur/kg bw.

CNCs attenuate the progression of cholangiocarcinoma in hamsters

It is known that *N*-nitrosodimethylamine treatment combined with liver-fluke infection causes both hepatocellular carcinoma and cholangiocarcinoma (Mitacek et al. 1999; Thamavit et al. 1994). We therefore confirmed that CCA was present by detecting the expression of the bile-duct marker, cytokeratin 19 (CK 19). Expression of CK19 was observed in all tumor lesions. PCNA, proliferation cell nuclear antigen, was used to investigate cell-proliferation index and AFP was used to confirm pre-neoplastic lesions, as shown in brown color in cholangiofibrosis, but not in CCA. Periodic acid-Schiff (PAS) stain was used to confirm mucin in cholangiofibrosis (Fig. 4). PCNA expression was significantly greater in ON and BNC treatment groups compared to normal controls. Its expression and distribution was significantly lower in both CNCs treatment groups, and especially in the 10 mg cur/kg bw group.

It is well known that chronic inflammation-mediated DNA damage is a key molecular mechanism of CCA genesis in OV-associated CCA (Pinlaor et al. 2005). We therefore investigated the expression of high mobility group box-1 (HMGB1), an inflammatory marker associated with carcinogenesis, which is a potential therapeutic target for cancers (Vijayakumar et al. 2019). HMGB1 expression was mainly observed in the nucleus of bile-duct epithelial cells and was highest in the ON and ON + BNC groups. In contrast, HMGB1 expression was significantly lower in the CNCs treatment groups (both 10 and 20 mg cur/kg bw) compared to the ON group in Fig. 6. Expression levels of CK-19 and AFP also supported these findings.

CNCs suppress the expression of oncogenic transcription factors-involved in cholangiogenesis

The effect of CNCs on the expression of oncogenic transcription factor NF-kB (65 kDa) and FOXM1 (110 kDa) are shown in Fig. 7. Western-blot analysis showed that expression of both was greater in the ON group compared to normal controls but was lower in groups treated with CNCs at both 10 and 20 mg cur/kg bw.

Discussion

In this study, we used an improved version of curcumin-loaded nanocomplexes (CNCs), known to be safe in mouse and hamster models (Jantawong et al. 2021) and with low cytotoxicity to normal fibroblast and cholangiocarcinoma cell lines (Pinlaor S et al. 2021). These CNCs were tested for their ability to retard CCA development in hamsters. Relative to controls, oral administration of CNCs with curcumin equivalent to 10 and 20 mg/kg bw thrice a week for five months increased survival rate of animals, reduced inflammation, reduced percentage of hamsters with CCA, reduced serum alkaline phosphatase levels and improved the histopathological picture. This was especially the case for treatment with CNCs at 10 mg cur/ kg bw. These effects may be exerted via suppression of PCNA, HMGB1, NF-kB and FOXM1. The consequence of histopathological changes by which CNCs suppress CCA induced by a combination of *O. viverrini* infection and *N*-nitrosodimethylamine treatment is summarized in Fig. 8.

Previous study demonstrated that native curcumin inhibits cholangiocarcinogenesis in our hamster/CCA model (Prakobwong et al. 2011b). CNCs exhibit anti-periductal fibrosis effects and could prevent bile canalicular abnormalities in *O. viverrini*-infected hamsters (Charoensuk et al. 2016). To gain better control of the delivery of curcumin, CNCs were further enhanced by using a solid-dispersion method with gums. Gum-based nanocarriers served as important containers for the protection and delivery of some active compounds (Taheri and Jafari 2019). Importantly, these polysaccharides cannot be digested/degraded in strong acid condition such as in the stomach and small intestine, but are degraded in the colon by colonic bacteria (Salyers et al. 1977). Therefore, use of arabic and xanthan gums for curcumin delivery could prevent curcumin release and degradation in the stomach and small intestine, but ensure release in the colon instead (Ribeiro et al. 2016; Srikaeo et al. 2018; Taheri and Jafari 2019).

Many cancers, including *O. viverrini*-associated CCA, arise from infection through chronic irritation and inflammation (Kawanishi et al. 2006; Yongvanit et al. 2012). These in turn can lead to cholangiofibrosis, nodular cholangiofibrosis or cholangiofibroma and contribute to CCA development (Bannasch 2019; Chen et al. 2019; Thoolen et al. 2010). The glandular epitheliam of both cholangiofibrosis and cholangiofibroma are typically lined with a simple layer of cuboidal or columnar cells. Generally, CK19 usually express in ductal epithelium such as bile epithelium duct, pancreas and also found in primitive hepatic progenitor cells. However, the CK19 expression is disappear in mature hepatocytes, but still present in bile duct epithelial. These is reason use CK19 to marker of bile duct epithelial in liver tissue (Leelawat et al. 2012; Zhuo et al. 2020). In hamsters and rats, cholangiofibrosis and cholangiofibroma have been considered as precursor lesions of CCA (Bannasch 2019). Hamsters in the ON and ON + BNCs groups after five months usually exhibited chronic inflammation, lead to cholangiofibroma, developing in some cases into solid mass lesions of CCA. In contrast, hamsters treated with CNCs of either concentration had lower chronic active inflammation scores both for the perihilar bile duct and the peripheral bile duct, suggesting the anti-inflammation potential of curcumin (Razavi et al. 2021). In particular, hamsters given CNCs at the dose rate of 10 mg cur/kg bw showed increased cholangiofibrosis, but a decrease of cholangiofibroma and CCA, while the opposite was apparent in the ON and ON + BNC groups. Hamsters given CNCs at 10 mg cur/kg bw were less likely to have CCA after five months: however, they still displayed cholangiofibrosis, a pre-neoplastic lesion. This implies that CNCs have the potential to delay CCA development by inhibiting chronic inflammatory processes at an initial step.

Adverse effects appear to have occurred in the group given a high-dose treatment (ON + CNCs 20 mg cur/kg bw). This may be due to an overdose of curcumin. This substance exerts pro-oxidant activity (Aggeli et al. 2013) and promotes gallbladder contraction (Rasyid et al. 2002) to release bile, as well as having an influence on bile flow (Wang et al. 2016) despite obstructions where adult *O. viverrini* occur, leading to increased bile-duct proliferation. This suggests that dosage of CNCs should be considered carefully in diseases associated with biliary obstruction. The beneficial effect of a low-dose CNCs treatment is in general agreement with a previous study in which a high dose of turmeric extract reduced inflammation (Boonjaraspinyo et al. 2009), and an appropriate curcumin dose reduced oxidative and nitrative DNA damage (Pinlaor et al. 2009), periductal fibrosis (Pinlaor et al. 2010) and prevented alteration of bile canaliculi in hamsters with opisthorchiasis.

CNCs may retard CCA progression via the antiproliferation effect of curcumin on CCA (Prakobwong et al. 2011a) and the suppression of inflammation-mediated molecular events related to multistep carcinogenesis (Prakobwong et al. 2011b). Here, we found that CNCs treatment reduced expression of HMGB1, NF-kB, PCNA and FOXM1 in CCA hamsters. Upregulation of NF-kB (Dolcet et al. 2005), FOXM1 (Wierstra 2013) and HMGB1 (Vijayakumar et al. 2019) is involved in tumorigenesis of different cancer types, influencing processes ranging from development to drug resistance. For this reason, these molecules have been targeted for cancer therapy. Suppression of NF-kB (Prakobwong et al. 2011a; Prakobwong et al. 2011b), FOXM1 (Zhang et al. 2014), PCNA (Prakobwong et al. 2011b) and HMGB1 (Wang et al. 2012) by curcumin that we noted was similar to many previous reports. Suppression of CCA development by curcumin might also be through targeting multiple proteins involved in CCA genesis (Khoontawad et al. 2018). In addition to suppression of CCA development, CNCs treatment could prevent liver damage, as evidenced by the decreased serum activity of ALT and AST and a reduction of HMGB-1 expression. Inhibition of the translocation and extracellular release of HMGB1 alleviates liver damage and fibrotic lesions (Bai et al. 2016). However, the specific mechanisms involved require further study.

In Conclusion

We further evaluated the effect of CNCs on opisthorchiasis-associated CCA in hamsters. CNCs, solid dispersion of curcumin-loaded nanoparticles, exhibit greater efficacy to delay CCA development than does straight curcumin. Treatment with CNCs increased survival in animals, reduced tumor development, reduced bile-duct injury and suppressed expression of NF-kB, FOXM1 and HMGB1. Based on our experiments, we suggest that CNCs at 10 mg cur/kg bw thrice a week is a promising dose rate for alleviation of CCA development in patients. CNCs, 35.71 mg/kg bw (equivalent to 10 mg cur/kg bw), as an effective dose to suppress CCA development, could be converted to a dose for clinical trials in patients at 28.95 mg/kg bw (an individual weighing 60 kg, dividing the human equivalent dose by 10-fold safety factor) of CNCs.

Abbreviations

CCA: cholangiocarcinoma; OV: *Opisthorchis viverrini*; CNCs: curcumin-loaded nanocomplexes; BNCs: blank nanocomplexes; cur: curcumin; CK19: cytokeratin 19; AFP: alpha fetoprotein; PCNA: proliferating cell nuclear antigen; HMGB1: high mobility group box 1; NF-kB: *Nuclear factor kappa B*; FOXM1: Forkhead Box

M1.

Declarations

Acknowledgements

We would like to thank Welltech Biotechnology Co., Ltd, Thailand for producing CNCs, and BNCs. We also acknowledge Mr. Suwit Balthaisong, Mr. Chitsakul Phuyao and Mrs. Em-orn Phanomsri from Department of Pathology, Faculty of Medicine, Khon Kaen University, Thailand for their help with staining sections using H&E and AFP. We also thank Prof. David Blair for invaluable suggestions and editing the manuscript via publication clinic, Khon Kaen University, Thailand.

Authors' contributions

SP: Project administration; Supervision; Data curation; Writing - review & editing. CJ: Methodology; Data curation; Writing - original draft. YC, CP and KI: Supervision; Methodology; Data curation; Writing - review & editing. AP: Resources; Supervision; Writing - review & editing. RD, TP, PP and SW: Methodology; Data curation; Writing - original draft.

Funding

This study was supported by Center of Excellence on Medical Biotechnology (CEMB), S&T Postgraduate Education and Research Development Office (PERDO), Office of Higher Education Commission (OHEC), Thailand (No. SN-59-002-05). CJ acknowledges the Cholangiocarcinoma Research Institute (CARI), Khon Kaen University, Khon Kaen, Thailand (No. CARI 02/2561).

Availability of data and materials

Not applicable.

Ethics approval and consent to participate

This study protocol was reviewed and approved by the Animal Ethics Committee of Khon Kaen University (ACUC-KKU-59/2559), based on the ethical guidelines for Animal Experimentation of the National Research Council of Thailand.

Consent for publication

Not applicable.

Competing interests

Welltech Biotechnology Co., Ltd, Thailand, the producer and supplier of CNCs and BNCs, had no part in the planning and conducting the experimental design in this project. The authors declare that they have no competing of interests.

References

1. Aggeli I K, E Koustas, C Gaitanaki, I Beis (2013) Curcumin acts as a pro-oxidant inducing apoptosis via JNKs in the isolated perfused Rana ridibunda heart. J Exp Zool A Ecol Genet Physiol 319(6):328–339
2. Anand P, A B Kunnumakkara, R A Newman, B B Aggarwal (2007) Bioavailability of curcumin: problems and promises. Mol Pharm 4(6):807–818
3. Bai L, M Kong, Q Zheng, X Zhang, X Liu, K Zu. et al (2016) Inhibition of the translocation and extracellular release of high-mobility group box 1 alleviates liver damage in fibrotic mice in response to D-galactosamine/lipopolysaccharide challenge. Mol Med Rep 13(5):3835–3841
4. Baker M (2017) Deceptive curcumin offers cautionary tale for chemists. Nature 541(7636):144–145
5. Banales J M, J J G Marin, A Lamarca, P M Rodrigues, S A Khan, L R Roberts. et al (2020) Cholangiocarcinoma 2020: the next horizon in mechanisms and management. Nat Rev Gastroenterol Hepatol 17(9):557–588
6. Bannasch P (2019) Letter to the Editor Regarding "Cholangiofibrosis and Related Cholangiocellular Neoplasms in Rodents". Toxicol Pathol 47(7):896–898
7. Boonjaraspinyo S, T Boonmars, C Aromdee, T Srisawangwong, B Kaewsamut, S Pinlaor. et al (2009) Turmeric reduces inflammatory cells in hamster opisthorchiasis. Parasitol Res 105(5):1459–1463
8. Carlsson G, B Gullberg, L Hafstrom (1983) Estimation of liver tumor volume using different formulas - an experimental study in rats. J Cancer Res Clin Oncol 105(1):20–23
9. Charoensuk L, P Pinlaor, S Wanichwecharungruang, K Intuyod, K Vaeteewoottacharn, A Chaidee. et al (2016) Nanoencapsulated curcumin and praziquantel treatment reduces periductal fibrosis and attenuates bile canalicular abnormalities in Opisthorchis viverrini-infected hamsters. Nanomedicine 12(1):21–32
10. Chen T, K Chen, S Qiu, P C Mann (2019) Spontaneous Cholangiofibrosis in a Wistar Rat. Toxicol Pathol 47(4):556–560
11. Dolcet X, D Llobet, J Pallares, X Matias-Guiu (2005) NF-kB in development and progression of human cancer. Virchows Arch 446(5):475–482
12. IARC (2012) A review of human carcinogens: *Opisthorchis viverrini* and *Clonorchis sinensis*. IARC Monogr Eval Carcinog Risks Hum 100B:341–370

13. Ipar V S, A Dsouza, P V Devarajan (2019) Enhancing Curcumin Oral Bioavailability Through Nanoformulations. Eur J Drug Metab Pharmacokinet 44(4):459–480
14. Jantawong C, A Priprem, K Intuyod, C Pairojkul, P Pinlaor, S Waraasawapati. et al (2021) Curcumin-loaded nanocomplexes: Acute and chronic toxicity studies in mice and hamsters. Toxicol Rep 8:1346–1357
15. Kawanishi S, Y Hiraku, S Pinlaor, N Ma (2006) Oxidative and nitrative DNA damage in animals and patients with inflammatory diseases in relation to inflammation-related carcinogenesis. Biol Chem 387(4):365–372
16. Khoontawad J, K Intuyod, R Rucksaken, N Hongsrichan, C Pairojkul, P Pinlaor. et al (2018) Discovering proteins for chemoprevention and chemotherapy by curcumin in liver fluke infection-induced bile duct cancer. PLoS One 13(11):e0207405
17. Lee J H, H J Rim, S Sell (1997) Heterogeneity of the "oval-cell" response in the hamster liver during cholangiocarcinogenesis following Clonorchis sinensis infection and dimethylnitrosamine treatment. J Hepatol 26(6):1313–1323
18. Leelawat K, S Narong, W Udomchaiprasertkul, J Wannaprasert, S A Treepongkaruna, S Subwongcharoen. et al (2012) Prognostic relevance of circulating CK19 mRNA in advanced malignant biliary tract diseases. World J Gastroenterol 18(2):175–181
19. Liu W, Y Zhai, X Heng, F Y Che, W Chen, D Sun. et al (2016) Oral bioavailability of curcumin: problems and advancements. J Drug Target 24(8):694–702
20. Mahran R I, M M Hagras, D Sun, D E Brenner (2017) Bringing Curcumin to the Clinic in Cancer Prevention: a Review of Strategies to Enhance Bioavailability and Efficacy. AAPS J 19(1):54–81
21. Mansouri K, S Rasoulpoor, A Daneshkhah, S Abolfathi, N Salari, M Mohammadi. et al (2020) Clinical effects of curcumin in enhancing cancer therapy: A systematic review. BMC Cancer 20(1):791
22. Mitacek E J, K D Brunnemann, M Suttajit, N Martin, T Limsila, H Ohshima. et al (1999) Exposure to N-nitroso compounds in a population of high liver cancer regions in Thailand: volatile nitrosamine (VNA) levels in Thai food. Food Chem Toxicol 37(4):297–305
23. Narama I, K Imaida, H Iwata, D Nakae, A Nishikawa, T Harada (2003) A review of nomenclature and diagnostic criteria for proliferative lesions in the liver of rats by a working group of the japanese society of toxicologic pathology. J Toxicol Pathol 16:1–17
24. Pinlaor S, Jantawong C, Intuyod K, Sirijindalert T, Pinlaor P, Pairojkul C. et al (2021) Solid dispersion improves release of curcumin from nanoparticles: Potential benefit for intestinal absorption. Mater Today Commun 26:1–9
25. Pinlaor S, S Prakobwong, Y Hiraku, P Pinlaor, U Laothong, P Yongvanit (2010) Reduction of periductal fibrosis in liver fluke-infected hamsters after long-term curcumin treatment. Eur J Pharmacol 638(1–3):134–141
26. Pinlaor S, B Sripa, N Ma, Y Hiraku, P Yongvanit, S Wongkham. et al (2005) Nitrative and oxidative DNA damage in intrahepatic cholangiocarcinoma patients in relation to tumor invasion. World J Gastroenterol 11(30):4644–4649
27. Pinlaor S, P Yongvanit, S Prakobwong, B Kaewsamut, J Khoontawad, P Pinlaor. et al (2009) Curcumin reduces oxidative and nitrative DNA damage through balancing of oxidant-antioxidant status in hamsters infected with Opisthorchis viverrini. Mol Nutr Food Res 53(10):1316–1328
28. Prakobwong S, S C Gupta, J H Kim, B Sung, P Pinlaor, Y Hiraku. et al (2011a) Curcumin suppresses proliferation and induces apoptosis in human biliary cancer cells through modulation of multiple cell signaling pathways. Carcinogenesis 32(9):1372–1380
29. Prakobwong S, J Khoontawad, P Yongvanit, C Pairojkul, Y Hiraku, P Sithithaworn. et al (2011b) Curcumin decreases cholangiocarcinogenesis in hamsters by suppressing inflammation-mediated molecular events related to multistep carcinogenesis. Int J Cancer 129(1):88–100
30. Prakobwong S, P Yongvanit, Y Hiraku, C Pairojkul, P Sithithaworn, P Pinlaor. et al (2010) Involvement of MMP-9 in peribiliary fibrosis and cholangiocarcinogenesis via Rac1-dependent DNA damage in a hamster model. Int J Cancer 127(11):2576–2587
31. Prueksapanich P, P Piyachaturawat, P Aumpansub, W Ridtitid, R Chaiteerakij, R Rerknimitr (2018) Liver Fluke-Associated Biliary Tract Cancer. Gut Liver 12(3):236–245
32. Rafiee Z, M Nejatian, M Daeihamed, S M Jafari (2019) Application of different nanocarriers for encapsulation of curcumin. Crit Rev Food Sci Nutr 59(21):3468–3497
33. Rasyid A, A R Rahman, K Jaalam, A Lelo (2002) Effect of different curcumin dosages on human gall bladder. Asia Pac J Clin Nutr 11(4):314–318
34. Razavi B M, M Ghasemzadeh Rahbardar, H Hosseinzadeh (2021) A review of therapeutic potentials of turmeric (Curcuma longa) and its active constituent, curcumin, on inflammatory disorders, pain, and their related patents. Phytother Res 35(12):6489–6513
35. Ribeiro A J, F R L de Souza, J Bezerra, C Oliveira, D Nadvorny, M F de La Roca Soares. et al (2016) Gums' based delivery systems: Review on cashew gum and its derivatives. Carbohydr Polym 147:188–200
36. Salyers A A, J R Vercellotti, S E West, T D Wilkins (1977) Fermentation of mucin and plant polysaccharides by strains of Bacteroides from the human colon. Appl Environ Microbiol 33(2):319–322
37. Shehzad A, F Wahid, Y S Lee (2010) Curcumin in cancer chemoprevention: molecular targets, pharmacokinetics, bioavailability, and clinical trials. Arch Pharm (Weinheim) 343(9):489–499
38. Shin H R, J K Oh, E Masuyer, M P Curado, V Bouvard, Y Y Fang. et al (2010) Epidemiology of cholangiocarcinoma: an update focusing on risk factors. Cancer Sci 101(3):579–585
39. Sirica A E, G J Gores, J D Groopman, F M Selaru, M Strazzabosco, X Wei Wang. et al (2019) Intrahepatic Cholangiocarcinoma: Continuing Challenges and Translational Advances. Hepatology 69(4):1803–1815
40. Sriamporn S, P Pisani, V Pipitgool, K Suwanrungruang, S Kamsa-ard, D M Parkin (2004) Prevalence of Opisthorchis viverrini infection and incidence of cholangiocarcinoma in Khon Kaen, Northeast Thailand. Trop Med Int Health 9(5):588–594

41. Srikaeo K, P Laothongsan, C Lerdluksamee (2018) Effects of gums on physical properties, microstructure and starch digestibility of dried-natural fermented rice noodles. Int J Biol Macromol 109:517–523
42. Sripa B, S Tangkawattana, P J Brindley (2018) Update on Pathogenesis of Opisthorchiasis and Cholangiocarcinoma. Adv Parasitol 102:97–113
43. Suwannateep N, W Banlunara, S P Wanichwecharungruang, K Chiablaem, K Lirdprapamongkol, J Svasti (2011) Mucoadhesive curcumin nanospheres: biological activity, adhesion to stomach mucosa and release of curcumin into the circulation. J Control Release 151(2):176–182
44. Taheri A, S M Jafari (2019) Gum-based nanocarriers for the protection and delivery of food bioactive compounds. Adv Colloid Interface Sci 269:277–295
45. Thamavit W, R Kongkanuntn, D Tiwawech, M A Moore (1987) Level of Opisthorchis infestation and carcinogen dose-dependence of cholangiocarcinoma induction in Syrian golden hamsters. Virchows Arch B Cell Pathol Incl Mol Pathol 54(1):52–58
46. Thamavit W, C Pairojkul, D Tiwawech, T Shirai, N Ito (1994) Strong promoting effect of Opisthorchis viverrini infection on dimethylnitrosamine-initiated hamster liver. Cancer Lett 78(1–3):121–125
47. Thoolen B, R R Maronpot, T Harada, A Nyska, C Rousseaux, T Nolte. et al (2010) Proliferative and nonproliferative lesions of the rat and mouse hepatobiliary system. Toxicol Pathol 38(7 Suppl):5S-81S
48. van Tong H, P J Brindley, C G Meyer, T P Velavan (2017) Parasite Infection, Carcinogenesis and Human Malignancy. EBioMedicine 15:12–23
49. Vijayakumar E C, L K Bhatt, K S Prabhavalkar (2019) High Mobility Group Box-1 (HMGB1): A Potential Target in Therapeutics. Curr Drug Targets 20(14):1474–1485
50. Wang C, H Nie, K Li, Y X Zhang, F Yang, C B Li. et al (2012) Curcumin inhibits HMGB1 releasing and attenuates concanavalin A-induced hepatitis in mice. Eur J Pharmacol 697(1–3):152–157
51. Wang Y, L Wang, X Zhu, D Wang, X Li (2016) Choleretic Activity of Turmeric and its Active Ingredients. J Food Sci 81(7):H1800-1806
52. Waraasawapati S, R Deenonpoe, P Sa-ngiamwibool, Y Chamgramol, C Pairojkul. 2021. Fluke-Associated Cholangiocarcinoma: A Regional Epidemic. In: Tabibian JH, editor. Diagnosis and Management of Cholangiocarcinoma. Switzerland: Springer. p 265–289.
53. Wierstra I (2013) FOXM1 (Forkhead box M1) in tumorigenesis: overexpression in human cancer, implication in tumorigenesis, oncogenic functions, tumor-suppressive properties, and target of anticancer therapy. Adv Cancer Res 119:191–419
54. Yongvanit P, S Pinlaor, H Bartsch (2012) Oxidative and nitrative DNA damage: key events in opisthorchiasis-induced carcinogenesis. Parasitol Int 61(1):130–135
55. Zhang J R, F Lu, T Lu, W H Dong, P Li, N Liu. et al (2014) Inactivation of FoxM1 transcription factor contributes to curcumin-induced inhibition of survival, angiogenesis, and chemosensitivity in acute myeloid leukemia cells. J Mol Med (Berl) 92(12):1319–1330
56. Zhang Y, A Rauf Khan, M Fu, Y Zhai, J Ji, L Bobrovskaya. et al (2019) Advances in curcumin-loaded nanopreparations: improving bioavailability and overcoming inherent drawbacks. J Drug Target:1–32
57. Zhuo J Y, D Lu, W Y Tan, S S Zheng, Y Q Shen, X Xu (2020) CK19-positive Hepatocellular Carcinoma is a Characteristic Subtype. J Cancer 11(17):5069–5077

Tables

Table 1. Changes in serum chemistry parameters after five months treatment with BNCs or CNCs thrice a week in hamsters in which CCA was induced by a combination of *Opisthorchis viverrini* infection and administration of a carcinogen.

Parameters	Reference range	Unit	Experimental groups				
			Normal	ON induced			
				Untreated (ON)	ON + BNCs	ON + CNCs 10 mg cur/kg bw	ON + CNCs 20 mg cur/kg bw
			n = 19	n = 12	n = 4	n = 10	n = 8
Total protein	4.5-7.5	g/dL	6.04±0.27	5.98±0.43	5.55±0.60	6.00±0.27	6.08±0.55
Albumin	2.3-4.3	g/dL	3.66±0.20	3.11±0.31*	2.70±0.92*	3.31±0.17@	3.10±0.40*
Globulin	2.3-4.3	g/dL	2.37±0.21	2.87±0.33*	2.85±0.40*	2.69±0.25*	2.98±0.27*
Total bilirubin	NA	mg/dL	0.03±0.05	0.22±0.16*	0.33±0.39*	0.26±0.21*	0.34±0.32*
ALT	22-128	U/L	54.53±19.23	272.64±105.95*	288.75±82.09*	261.13±113.86*	270.43±164.17*
AST	20-150	U/L	98.67±51.90	126.83±44.19	149.50±61.11	149.29±31.22	115.83±36.45
Alkaline phosphatase	50-186	U/L	68.21±30.85	100.17±23.84*	76.50±35.34	74.50±14.13	83.13±16.00

Note: BNCs – blank nanocomplexes; CNCs – Curcumin-loaded nanocomplexes; ON – a combination of *Opisthorchis viverrini* infection and administration of *N*-nitrosodimethylamine; mg cur/kg bw – mg curcumin/kg body weight. Data are mean ±SD and analyzed by one-way ANOVA. ***P*** value < 0.05 compared to

normal group, #*P* value < 0.05 compared to ON untreated group, @*P* value < 0.05 compared to ON+BNC group, n = number of sacrificed animals at the end of experiment and used for biochemistry analysis. Data from animals dying before the end of the experiment were not analyzed. NA = not available.

Table 2. Histopathological findings in hamster livers

Experimental groups		Percentage survival rate (mean±SD)	Grading				CCA incidence	
			Chronic active inflammation score (mean±SD)		Cholangiofibrosis (mean±SD)	Cholangiofibroma (mean±SD)	Percent of hamsters developing CCA (No. of hamsters)	Tum volu (mea
			Perihilar bile duct	Peripheral bile duct				
Normal		95% (19/20)	0.00±0.00	0.00±0.00	0.00±0.00	0.00±0.00	0% (0/19)	0.00
ON induced	Untreated	40% (12/30)	4.40±0.84*	5.00±0.00*	2.30±2.06*	2.40±2.37*	50% (6/12)	47.3
	ON+BNCs	40% (4/10)	3.25±0.50*,#	4.50±0.58*	2.25±0.50*	3.50±2.38*	50% (2/4)	38.9
	ON+CNCs 10 mg cur/kg bw	66.67% (10/15)	2.70±0.67*,#	3.90±0.88*,#	2.70±1.83*	1.10±1.85	30% (3/10)	22.3
	ON+CNCs 20 mg cur/kg bw	53.33% (8/15)	2.63±0.92*,#	4.00±0.93*,#	2.88±1.13*	2.50±0.93*	75% (6/8)	33.4

Note: BNCs – blank nanocomplexes, CNCs – Curcumin-loaded nanocomplexes, ON – a combination of *Opisthorchis viverrini* infection and *N*-nitrosodimethylamine, Data are mean ±SD, **P* value < 0.05 compared to normal controls when analyzed by one-way ANOVA, #*P* value < 0.05 compared to ON untreated group when analyzed by one-way ANOVA

Figures

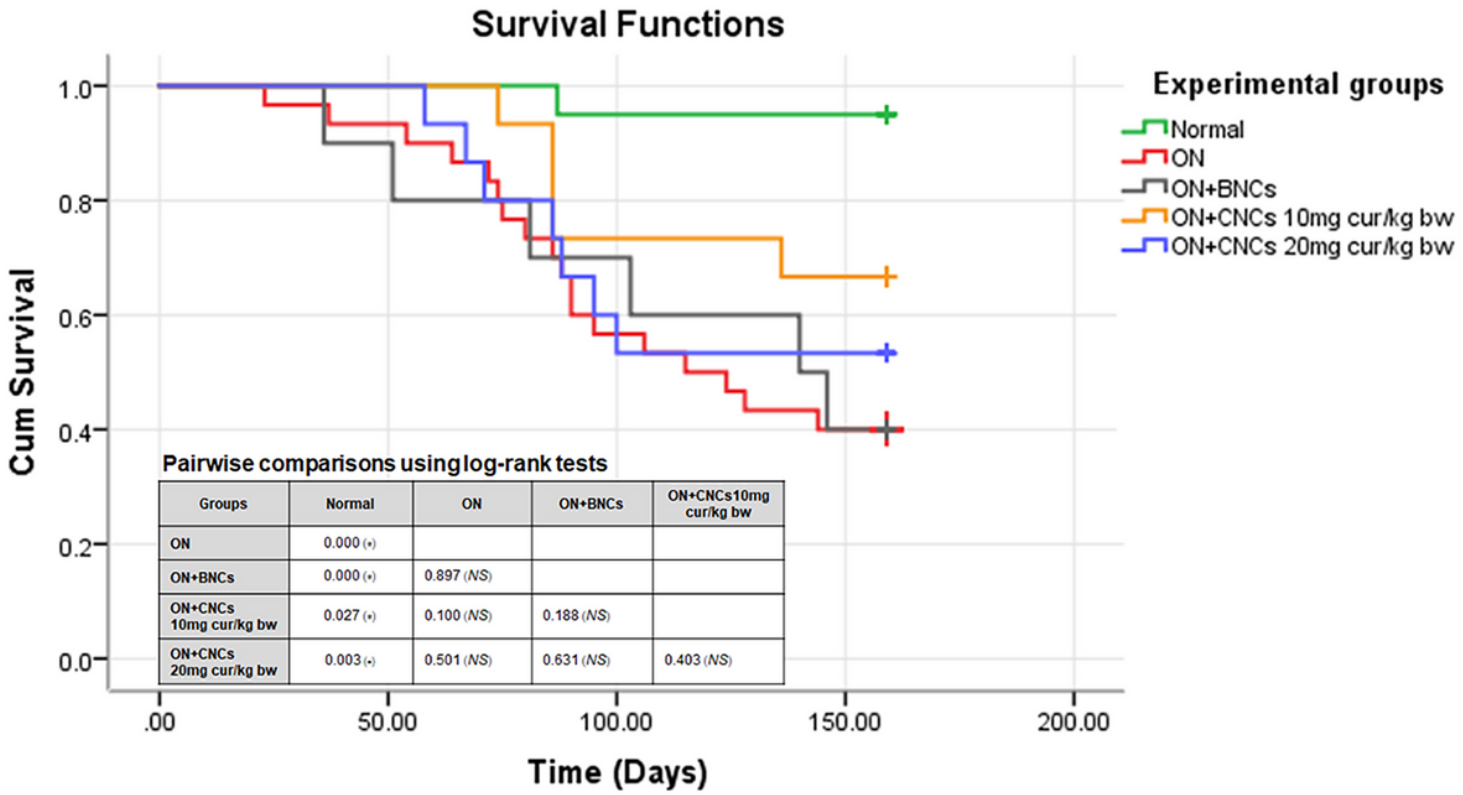

Figure 1

Kaplan-Meier plots of survival rates in animals. Hamsters were divided into five groups; normal controls (green), a combination of *Opisthorchis viverrini* infection and *N*-nitrosodimethylamine administration (ON, red), ON followed by administration of CNCs containing 10 mg curcumin/kg bw (ON+CNCs 10 mg, orange) and 20 mg curcumin/kg bw (ON+CNCs 20 mg, blue), and blank nanocomplexes (ON+BNCs, gray). CNCs and BNCs were administered thrice a week. Animal were maintained on these regimes for 5 months and survival was recorded daily.

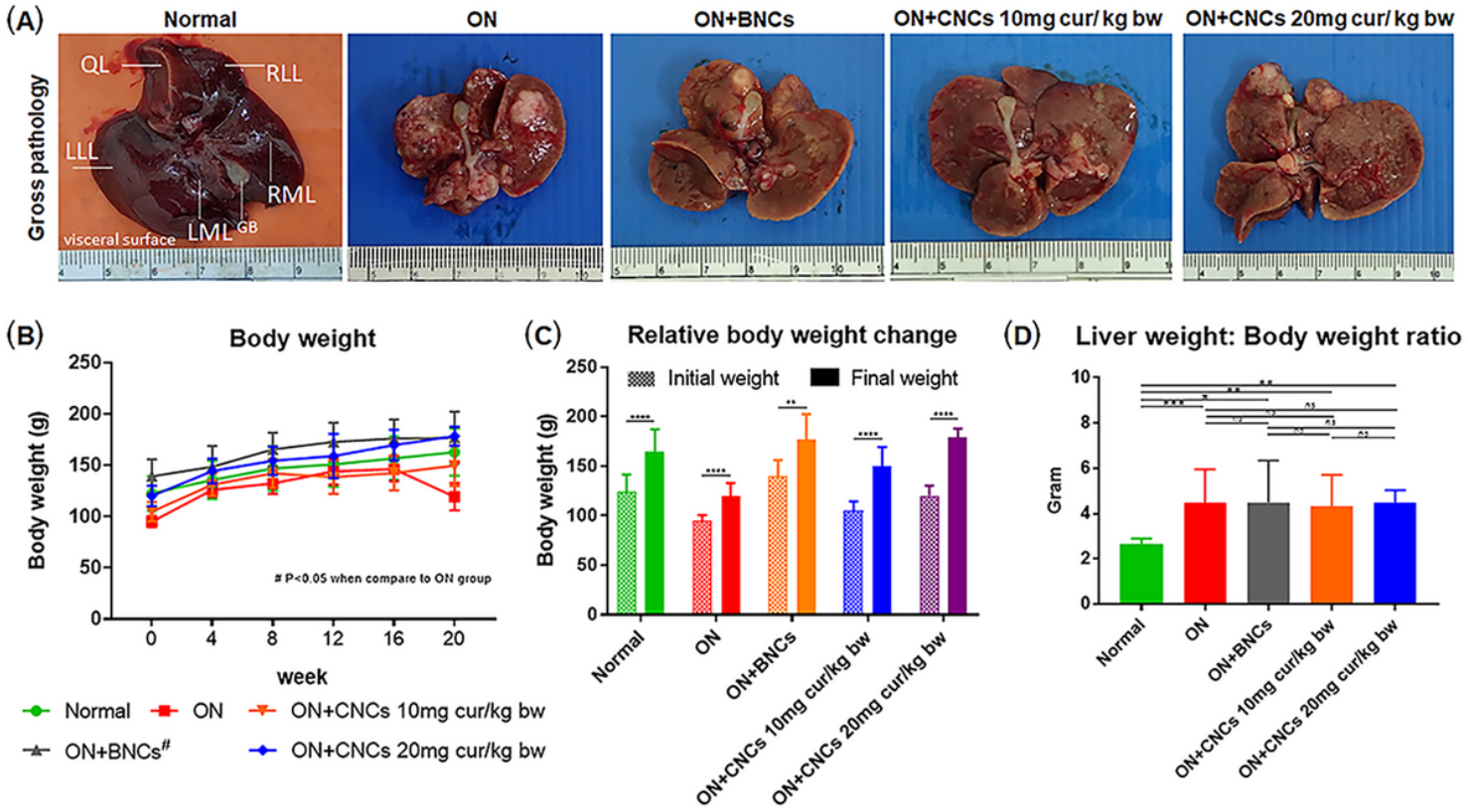

Figure 2

Development of CCA in hamsters was induced by a combination of *Opisthorchis viverrini* (OV) infection and *N*-nitrosodimethylamine (NDMA) using treatment thrice a week for five months. **(A)** Representative gross appearance. **(B)** Body-weight gain. **(C)** Relative body-weight change and **(D)** Liver weight per body weight (LW:BW) ratio in each experimental group at the end of five months. Experimental groups are identified in the legend for Fig. 1. QL = quadrate lobe, RLL = right lateral lobe, LLL = left lateral lobe, RML = right middle lobe, LML = left middle lobe, GB = gallbladder.

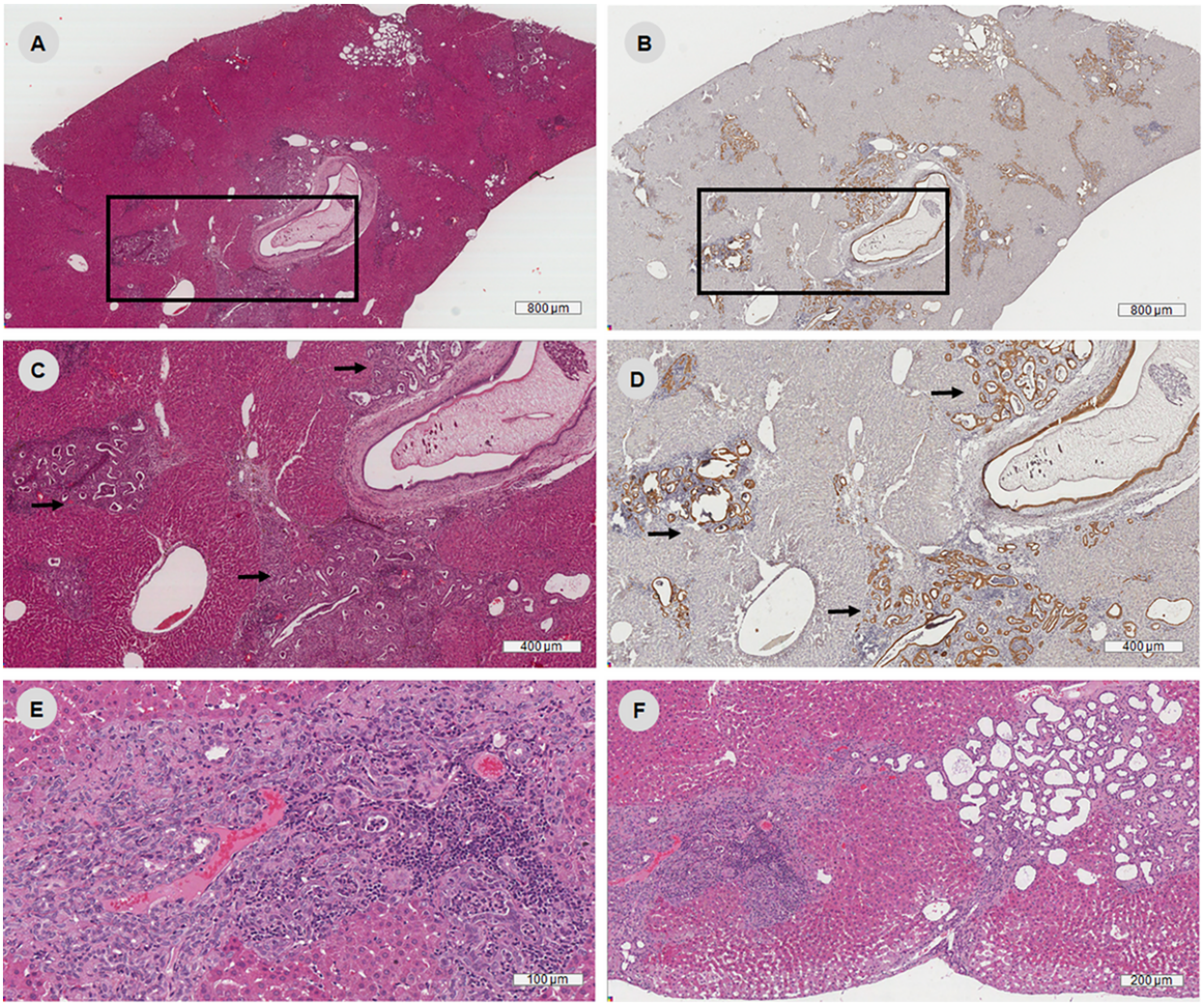

Figure 3

Micrographs of chronic active cholangitis in hamster livers with obstructive cholestasis from the group infected with *O. viverrini* and received NDMA, at 5 months. **(A, B)** overview of generalized cholangitis lesions in chronic obstructive cholestasis in opisthorchiasis, **(A)** H&E stain and **(B)** cytokeratin 19 **(A, B, inset)** indicted perihilar areas. **(C, D)** Chronic active cholangitis (black arrow) at perihilar area, **(C)** H&E stain and **(D)** cytokeratin 19. **(E)** Chronic active cholangitis of peripheral bile ducts at subcapsular area, showing inflammatory exudates in bile duct lumens and mixed inflammatory cell infiltration in periductal and interstitial tissue. **(F)** peripheral bile ducts at subcapsular area, **(F, left)** reveal chronic cholangitis and **(F, right)** healed cholangitis foci.

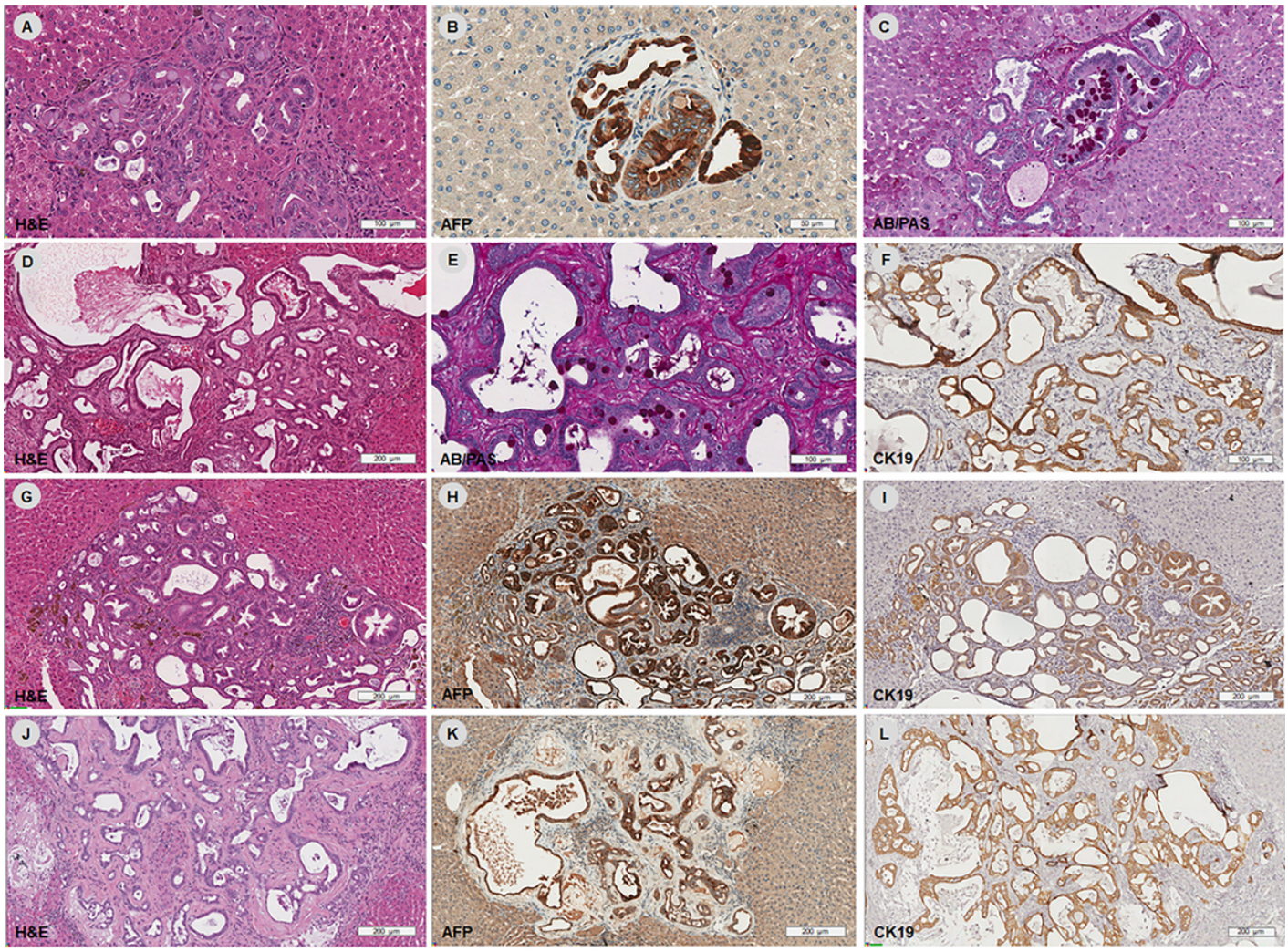

Figure 4

Representative micrographs of xenobiotic-induced cholangiofibrosis and cholangiofibroma in hamster livers with *O. viverrini* infection and receiving NDMA, after 5 months. **(A-C)** Early development of cholangiofibrosis, initially associated with oval-cell proliferation and bile-duct hyperplasia. **(A)** A lesion showing portal proliferation of bile ductules, lined by a single layer of cuboidal or columnar epithelium along with mucin-containing cells. **(B)** Ductular reaction cells are positive for AFP: a marker for bipotential oval cells. **(C)** AB/PAS: acid mucin was present in goblet cells (intestinal metaplasia). **(D-F)** Cholangiofibrosis consists of dilated to cystic bile ducts filled with mucus, cellular debris and surrounded by inflammatory cell infiltrates and connective tissue. **(E)** AB/PAS **(F)** CK 19 was present in both biliary gland and glands with intestinal metaplasia. **(G-I)** Cholangiofibrosis, progressing lesion. **(G)** There is aggregation of the adjacent portal lesions, as well as ductal proliferation and cystic dilatation of metaplastic glands, peribiliary fibrosis and a mixed inflammatory-cell infiltrate. **(H-I)** The lesion is positive for both AFP and CK19, indicating oval-cell proliferation and developed in the line of cholangiocytes. **(J-L)** Cholangiofibroma. **(J)** Cholangiofibroma, expanding nodular formation of glandular and stroma components of cholangiofibrosis. **(K-L)** The lesion is positive for both AFP and CK19, similar to cholangiofibrosis.

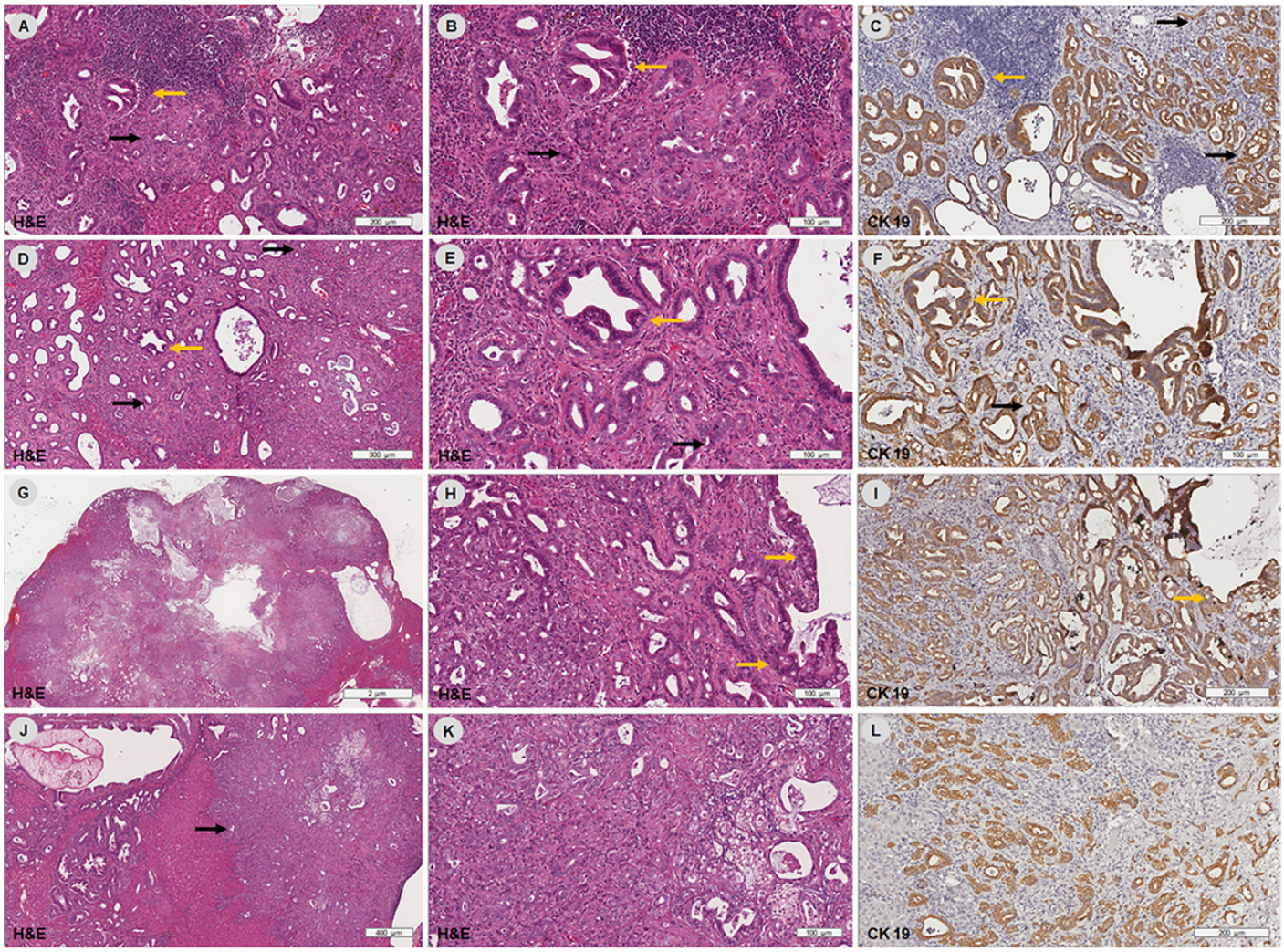

Figure 5

Representative micrographs of cholangiocarcinoma (CCA) and its precursor lesions in H&E stained sections. A primary lesion from the bile duct is indicated by CK19 staining, in hamster livers infected with *O. viverrini* and receiving NDMA, at 5 months.

(A-C) Malignant transformation of cholangiofibrosis; **(D-F)** Malignant transformation of cholangiofibroma; CCA (black arrow). Noted abnormal overlapping and *piling* up of *cells* and gland forming at a metaplastic duct (yellow arrow), with proliferation of atypical ductules in the hepatic parenchyma (black arrows). **(G-I)** CCA (black arrow), a well-differentiated adenocarcinoma producing mucin; malignant transformation from a dilated metaplastic duct (yellow arrow), is noted. **(J-L)** CCA (black arrow), a moderately differentiated adenocarcinoma with mild production of mucin, malignant transformation foci are obscured.

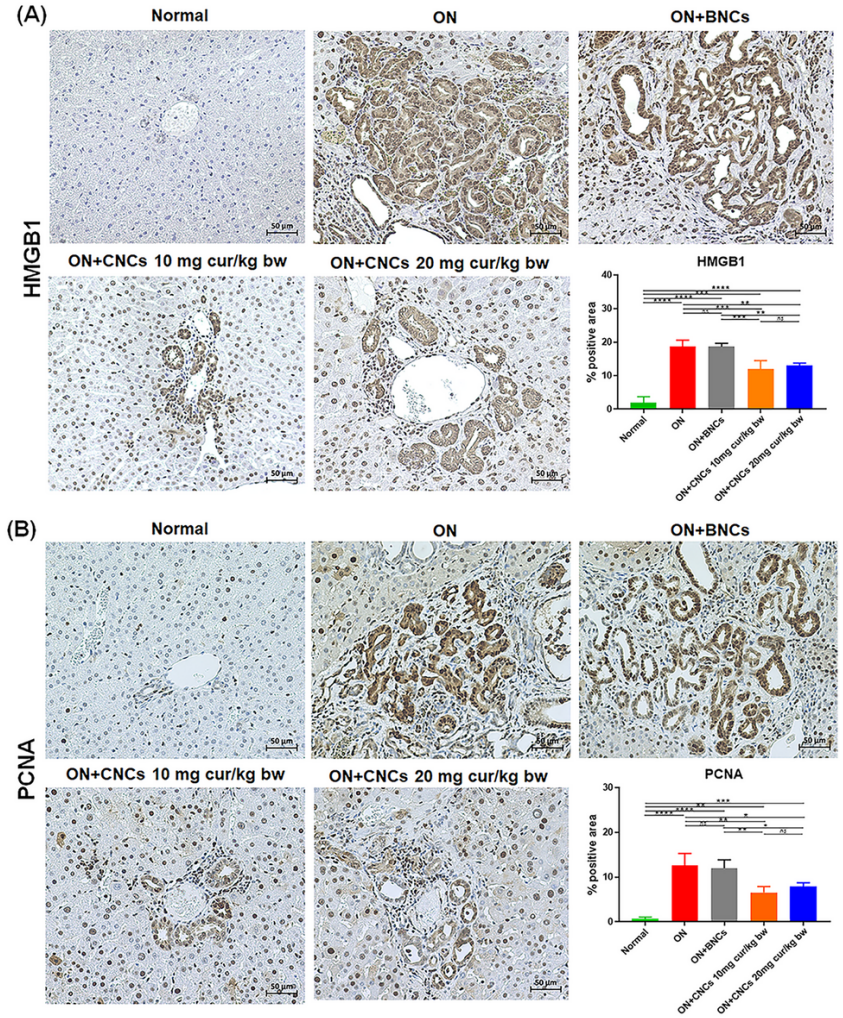

Figure 6

Representative images of liver sections using immunohistochemical staining. **(A)** HMGB1 and **(B)** PCNA expression in liver tissues of hamsters from all experimental groups and grading score in liver tissue.

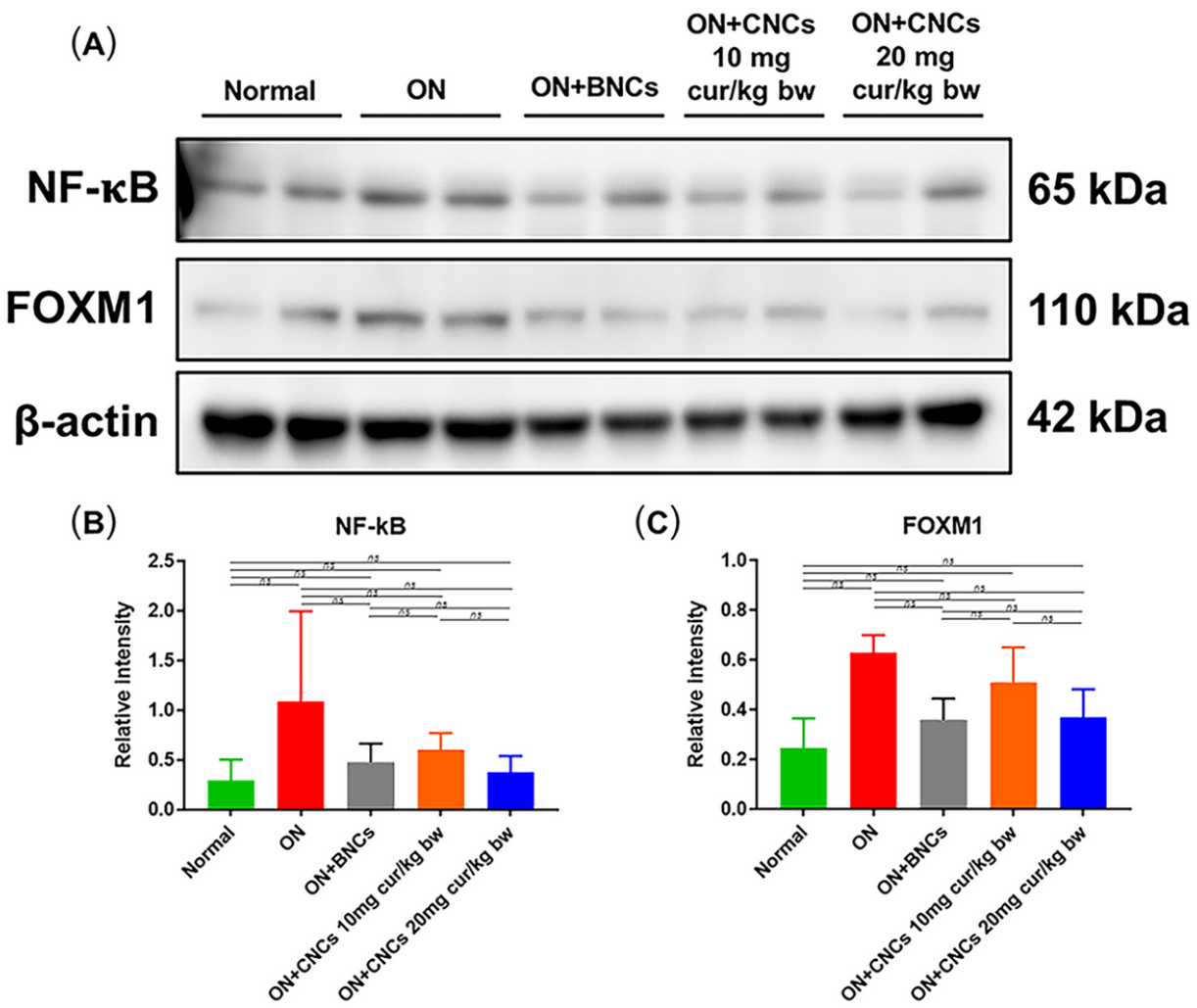

Figure 7

Effect of CNCs on expression of transcription factors NF-kB and FOXM1 in hamster livers. (A) NF-kB and FOXM1 protein expression was measured by western blot. (B, C) Relative intensity of protein bands and shown as a graph. All pairwise statistical comparisons were non-significant.

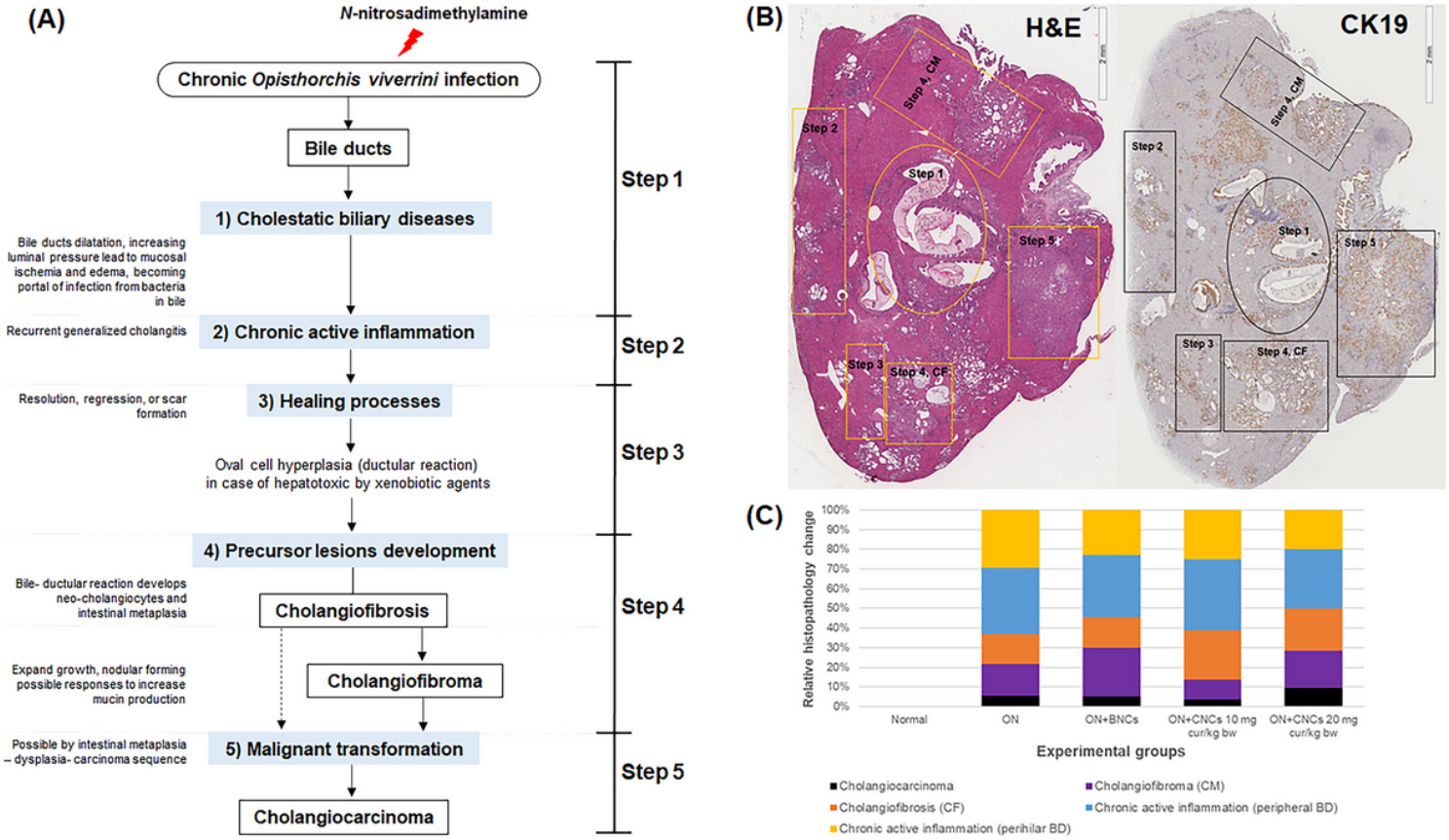

Figure 8

Summary of attenuation effects of curcumin-loaded nanocomplexes (CNCs) in hamsters with cholangiocarcinoma induced by *Opisthorchis viverrini* (OV) infection and *N*-nitrosadimethylamine (NDMA) treatment after 5 months. **(A)** Hypothetical pathway of cholangiocarcinogenesis induction by combination of OV plus NDMA in hamsters. **(B)** Areas mapped to demonstrate pathological steps 1-5 in (A), in a representative hamster liver. CF = cholangiofibrosis, CM = cholangiofibroma. **(C)** Comparison of relative histopathology observed in each experimental group.

Supplementary Files

This is a list of supplementary files associated with this preprint. Click to download.

- FigS1.tif
- FigS2.tif
- SupplementaryTable.docx